Computers and Chemical Engineering 33 (2009) 1336–1343

Contents lists available at ScienceDirect

Computers and Chemical Engineering

journal homepage: www.elsevier.com/locate/compchemeng

An efficient algorithm for rigorous dynamic simulation of reactive distillation columns

Mayur Rahul, M.V. Pavan Kumar, Deeptanshu Dwivedi, Nitin Kaistha*

Department of Chemical Engineering, Indian Institute of Technology Kanpur, Kanpur 208016, India

ARTICLE INFO

Article history:
Received 15 October 2008
Received in revised form 23 January 2009
Accepted 27 January 2009
Available online 4 February 2009

Keywords:
Reactive distillation
Rigorous dynamic simulation
Equilibrium reactive tray model

ABSTRACT

An efficient algorithm is developed for solving the system of differential algebraic equations (DAE) describing the dynamics of a reactive distillation (RD) column using the equilibrium tray model. Unlike existing algorithms, the rate of change of tray specific enthalpy is obtained analytically. This allows direct calculation of the instantaneous vapor rate leaving a tray from the dynamic energy balance. Application to an example methyl acetate RD column shows that the developed algorithm is twice as fast as the algorithm of Jhon and Lee [Jhon, Y. H., & Lee, T. H. (2003). Dynamic simulation for reactive distillation with ETBE synthesis. *Separation and Purification Technology*, *31*, 301–317].

1. Introduction

In reactive distillation (RD) systems, the reaction-separation interaction causes high non-linearity and there are several literature reports documenting the existence of steady-state multiplicity (see, e.g. Chen, Huss, Malone, & Doherty, 2002; Jacobs & Krishna, 1993; Mohl et al., 1999; Singh, Singh, Kumar, & Kaistha, 2005). In light of the high non-linearity, one of the key challenges in RD technology commercialization is the design of a robust control system that rejects large disturbances without succumbing to non-linear dynamic phenomena such as a steady-state transition (Kumar & Kaistha, 2008a). Control system design and validation through rigorous dynamic simulations is then an integral part the RD process design cycle with the most economical column design being modified, if necessary, to ensure good controllability (Georgiadis, Schenk, Pistikopoulos, & Gani, 2002).

The equilibrium tray model, where the vapor and liquid leaving a tray are assumed to be in equilibrium, is the bedrock of ordinary/reactive distillation column simulation (Seader & Henley, 1998). Even as the more sophisticated rate based non-equilibrium modeling approach (Baur, Taylor, & Krishna, 2001; Noeres, Kenig, & Górak, 2003) has gained prominence in recent years for RD systems, the equilibrium stage model remains widely used due to its relative simplicity and ability to capture the essential process behavior.

Rigorous dynamic simulation using the equilibrium tray model requires solving the tray dynamic material and energy balances along with the vapor–liquid equilibrium constraints. The resulting system of equations is a highly coupled set of differential algebraic equations (DAEs). Typically, in ordinary distillation systems, the tray dynamic energy balance is simplified by assuming that the rate of change of tray specific enthalpy is negligible. The resulting algebraic equation gives the unknown vapor rate leaving a tray providing the instantaneous vapor dynamics (Luyben, 1992). The dynamic component material balance equations are then integrated to the next time step. For reactive systems, since reaction heat effects are seldom negligible, constant tray specific enthalpy is a dubious assumption. To rigorously solve for the instantaneous vapor dynamics, Jhon and Lee (2003) proposed an iterative scheme to numerically estimate the rate of change of tray specific enthalpy and then calculate the instantaneous vapor rate leaving a tray from the dynamic energy balance. The iterations significantly slow down the simulation speed, particularly when the vapor–liquid equilibrium (VLE) is highly non-ideal since repeated bubble point calculations must be performed in the iterations.

In this work, using an approach similar to Howard (1970) for ordinary distillation systems, a direct non-iterative method for analytical calculation of the instantaneous vapor rate leaving an equilibrium reactive tray is developed. Application of the algorithm to simulate the open and closed loop dynamics of an example methyl acetate RD column demonstrates significant enhancement in computational speed over the state-of-the-art algorithm of Jhon and Lee (2003). The computational speed enhancement can significantly improve the performance of model predictive control and real-time optimization applications in RD systems. The major contribution of the work in relation to the work of Howard (1970) and Jhon and Lee (2003) is in the development of the significantly faster algorithm for solving the equilibrium *reactive* tray DAE model, its application to the highly non-linear methyl acetate RD system with

* Corresponding author. Tel.: +91 512 2597432; fax: +91 512 2590104.
E-mail address: nkaistha@iitk.ac.in (N. Kaistha).

0098-1354/$ – see front matter © 2009 Elsevier Ltd. All rights reserved.
doi:10.1016/j.compchemeng.2009.01.015

Nomenclature

Indices

i, k	component index, 1 to C
j	tray index, 1 to N, bottom-up tray numbering
n	reaction index, 1 to R

Symbols

g_j	function driven to zero for bubble point calculation on jth tray
h^L	liquid phase molar specific enthalpy
h^V	vapor phase molar specific enthalpy
$h_{ow,j}$	height of liquid over the weir at jth tray
$f_{i,j}$	ith component molar flow rate in feed to jth tray
$l_{i,j}$	ith component molar flow rate in liquid stream leaving jth tray
k	vapor phase acetic acid dimerization constant
l_w	length of weir
$r_{j,k}$	rate of kth reaction on jth tray
$u_{i,j}$	ith component hold-up in jth tray
$v_{i,j}$	ith component flow rate in vapor stream leaving jth tray
$x_{i,j}$	ith component mol fraction of liquid stream leaving jth tray
$y_{i,j}$	ith component mol fraction of vapor stream leaving jth tray
F_j	molar flow rate of feed to jth tray
L_j	molar flow rate of liquid stream leaving jth tray
U_j	total molar hold-up on jth tray
V_j	molar flow rate of vapor stream leaving jth tray
P	column pressure
P_i^{sat}	saturation pressure of ith component (from Antoine's equation)
T	temperature
W_j	catalyst weight on jth tray

Greek symbols

γ_i	liquid phase activity coefficient of ith component
$\nu_{i,k}$	stoichiometric coefficient of ith component in kth reaction
ρ	liquid density at jth tray
ξ_i	Marek's correction factor in VLE expression for ith component

complex VLE and systematic quantification of the computational speed enhancement.

2. RD dynamic simulation algorithm

2.1. Governing equations

Consider the schematic of a general reactive tray as in Fig. 1. Bottom-up tray numbering is used. Using conventional nomenclature, the dynamic component and total material balance equations for the tray, assuming the streams leaving a tray are at vapor–liquid equilibrium and neglecting the tray vapor hold-up, may be written as

$$\frac{dU_j x_{i,j}}{dt} = L_{j+1}x_{i,j+1} + V_{j-1}y_{i,j-1} + F_j z_{i,j} - L_j x_{i,j} - V_j x_{i,j} + \sum_{n=1}^{R} \nu_{i,n} r_{n,j} W_j \quad i = 1 \text{ to } C-1 \tag{1a}$$

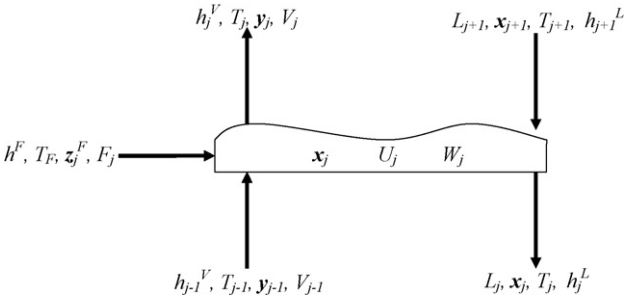

Fig. 1. Schematic of a reactive tray.

$$\frac{dU_j}{dt} = L_{j+1} + V_{j-1} + F_j - L_j - V_j + \sum_{n=1}^{R}\left(\sum_{i=1}^{C}\nu_{i,n}\right) r_{n,j}W_j \tag{1b}$$

Note that $W_j = 0$ for non-reactive trays in Eqs. (1a) and (1b) above. The dynamic energy balance for the tray is

$$\frac{dU_j h_j^L}{dt} = L_{j+1}h_{j+1}^L + V_{j-1}h_{j-1}^V + F_j h_j^F - L_j h_j^L - V_j h^V \tag{2a}$$

This equation is general and applicable to both reactive and non-reactive trays. An explicit term for the reaction heat released on a reactive tray does not occur in the equation since the specific molar enthalpies are obtained from heats of formation. Expanding the left hand side (LHS)

$$U_j\frac{dh_j^L}{dt} + h_j^L\frac{dU_j}{dt} = L_{j+1}h_{j+1}^L + V_{j-1}h_{j-1}^V + F_j h^F - L_j h_j^L - V_j h_j^V \tag{2b}$$

Substituting Eq. (1b) into (2b) and rearranging, we get

$$U_j\frac{dh_j^L}{dt} = L_{j+1}\left(h_{j+1}^L - h_j^L\right) + V_{j-1}\left(h_{j-1}^V - h_j^L\right) + F_j\left(h_j^F - h_j^L\right) - V_j\left(h_j^V - h_j^L\right) - h_j^L\sum_{n=1}^{R}\left(\sum_{i=1}^{C}\nu_{i,n}\right) r_{n,j}W_j \tag{2c}$$

The tray liquid hold-up and composition as well the state of all the inlet streams (vapor or liquid or feed) are known. Since the liquid and vapor leaving a tray are at equilibrium, a bubble point calculation at the known tray liquid composition and pressure gives the vapor phase composition, and temperature as well as its specific molar enthalpy from thermodynamic property equations. The specific molar liquid enthalpy leaving a tray is also calculated from the bubble tray temperature. The liquid flow rate leaving a tray is obtained from a tray liquid hydraulic equation such as the Francis Wier formula as

$$L_j = C\rho_j^L l_w h_{ow,j}^{1.5} \tag{3}$$

All the terms on the right hand side (RHS) of the tray material balance (Eqs. (1a) and (1b)) except the total vapor flow leaving the tray (V_j) are thus known.

To calculate V_j, consider the energy balance Eq. (2c). If dh_j^L/dt is set to zero, the equation can be solved to calculate V_j. It is however established that even for ordinary multi-component distillation systems, the vapor dynamics assuming $dh_j^L/dt = 0$ can differ significantly from rigorous dynamics accounting for dh_j^L/dt (Howard, 1970). Given that reaction heat effects are seldom negligible for RD systems, the effect of molar specific enthalpy change must be accounted for in the tray energy balance.

For a rigorous solution of the dynamic energy balance, Jhon and Lee (2003) proposed an iterative scheme where the material balance equation is integrated forward in time from t to $t+\Delta t$ for an assumed value of V_j. The specific liquid enthalpy ($h_j^L|_{t+\Delta t}$) is then

calculated from the bubble temperature at the liquid composition so obtained. A numerical estimate of the rate of change of tray specific enthalpy can then be obtained. Substituting this numerical estimate and the assumed V_j in Eq. (2c), the LHS and RHS must be equal if the assumed V_j is correct. The discrepancy is used to iteratively update V_j using the secant method. Note that a bubble point calculation must be performed for every iteration in V_j. Also a one-step forward integration of the material balance equations must be performed. To ensure quick convergence to the bubble temperature, its value at the previous time step is used as a good initial guess. Even so, for systems with highly non-ideal VLE, the repeated bubble point calculations and one-step forward material balance integration can significantly slow down the computation.

Instead of iteratively calculating V_j using a numerical approximation of dh_j^L/dt, direct analytical calculation of dh_j^L/dt would allow for obtaining V_j in a single step from Eq. (2c). The specific tray liquid enthalpy, h_j^L, is a function of the tray composition and temperature. Instead of working with the compositions which are constrained to sum to 1, it is convenient to consider h_j^L to be a function of the tray component hold-ups ($u_{i,j}$) with all tray component hold-ups being independent so that

$$h_j^L = h_j^L(x_j, T_j) = h_j^L(\boldsymbol{u}_j, T_j)$$

with

$$x_{i,j} = \frac{u_{i,j}}{\sum_{i=1}^{C} u_{i,j}} \tag{4a}$$

Differentiating with respect to time, we have

$$\frac{dh_j^L}{dt} = \frac{\partial h_j^L}{\partial T_j} \cdot \frac{dT_j}{dt} + \sum_{i=1}^{C} \frac{\partial h_j^L}{\partial u_{i,j}} \cdot \frac{du_{i,j}}{dt} \tag{4b}$$

or in succinct notation

$$\frac{dh_j^L}{dt} = h_{T_j}^L \cdot \frac{dT_j}{dt} + \sum_{i=1}^{C} h_{u_{i,j}}^L \cdot \frac{du_{i,j}}{dt} \tag{4c}$$

The thermodynamic expression for h_j^L can be differentiated with respect to T_j and $u_{i,j}$ to obtain analytical expressions for the partial derivatives in Eq. (4c) above. The total and component material balance in Eqs. (1a) and (1b) is reformulated in terms of the component hold-up ($u_{i,j}$) as

$$\frac{du_{i,j}}{dt} = L_{j+1}x_{i,j+1} + V_{j-1}y_{i,j-1} + F_j z_{i,j} - L_j x_{i,j} - V_j x_{i,j} + \sum_{n=1}^{R} \nu_{i,n} r_{n,j} W_j \quad i = 1 \text{ to } C \tag{5}$$

to obtain $du_{i,j}/dt$ in terms of the unknown V_j. An analytical expression for dT_j/dt is obtained from the fact that the tray is at the bubble point at every point in time. The bubble point temperature corresponds to that special value of the temperature for which the vapor phase compositions calculated from the equilibrium relation sum to 1. From the VLE expression

$$\gamma_{i,j} x_{i,j} P_{i,j}^{sat} = y_{i,j} P_j \quad i = 1 \text{ to } C \tag{6a}$$

we have at the bubble point temperature

$$g_j \equiv \sum_{i=1}^{C} \frac{\gamma_{i,j} x_{i,j} P_{i,j}^{sat}}{P_j} - 1 = 0 \tag{6b}$$

Since the tray is at the bubble point temperature at all times, we have

$$\frac{dg_j}{dt} = 0 \tag{7a}$$

Now

$$\frac{dg_j}{dt} = \sum_{i=1}^{C} g_{u_{i,j}} \frac{du_{i,j}}{dt} + g_{T_j} \frac{dT_j}{dt} \tag{7b}$$

Combining Eqs. (7a) and (7b), we get

$$\frac{dT_j}{dt} = -\frac{\sum_{i=1}^{C} g_{u_{i,j}} (du_{i,j}/dt)}{g_{T_j}} \tag{8}$$

Substitution of Eq. (8) above into Eq. (4c) gives dh_i^L/dt as a function $du_{i,j}/dt$. Replacing $du_{i,j}/dt$ from Eq. (5) and substituting into the energy balance equation (Eq. (2c)), we finally get after algebraic manipulations

$$V_j = \frac{L_{j+1}\alpha_{j+1}^L + V_{j-1}\alpha_{j-1}^V + F_j\alpha_j^F - \sum_i (h_j^L + \beta_{i,j} Uj) \sum_k \nu_{i,k} r_{k,j} W_j}{\alpha_j^V} \tag{9}$$

where

$$\beta_{i,j} = \frac{\partial h_j^L}{\partial u_{i,j}} - \frac{(\partial h_j^L/\partial T_j) \cdot (\partial g_j/\partial u_{i,j})}{\partial g_j/\partial T_j}$$

and

$$\alpha_{j+1}^L = h_{j+1}^L - h_j^L - U_j \sum_i \beta_{i,j} x_{i,j+1}$$

$$\alpha_{j-1}^V = h_{j-1}^V - h_j^L - U_j \sum_i \beta_{i,j} x_{i,j-1}$$

$$\alpha_j^F = h_j^F - h_j^L - U_j \sum_i \beta_{i,j} z_{i,j}^F$$

$$\alpha_j^V = h_j^V - h_j^L - U_j \sum_i \beta_i y_{i,j}$$

Eq. (9) gives the instantaneous vapor rate leaving a tray (V_j) as all quantities on the RHS are known. Once V_j is calculated, all the terms on the RHS of the dynamic material balance in Eqs. (1a) and (1b) are known which can then be integrated to the next time step. Note that, analytical expressions are used for calculating the partial derivatives in Eq. (9). From Fig. 1, V_j is an input stream to the next upper tray. This gives a bottom-up tray-by-tray calculation procedure where V_j is calculated for all the trays ($j = 0$ to N) and the dynamic material balance is integrated to the next time step. Fig. 2 contrasts the Jhon–Lee algorithm and the proposed algorithm for dynamic simulation of an RD column section with N trays.

The analytical partial derivative expressions are quite involved and depend on the equation-of-state used to model the VLE and the enthalpies. To ensure the expressions are correct for the methyl acetate RD system studied here, the partial derivatives from the expressions were matched to their numerically calculated values. It must be said that obtaining the correct analytical expression requires significant effort. This is however only a one-time exercise with the expressions being applicable to any other RD system using the same thermodynamic model.

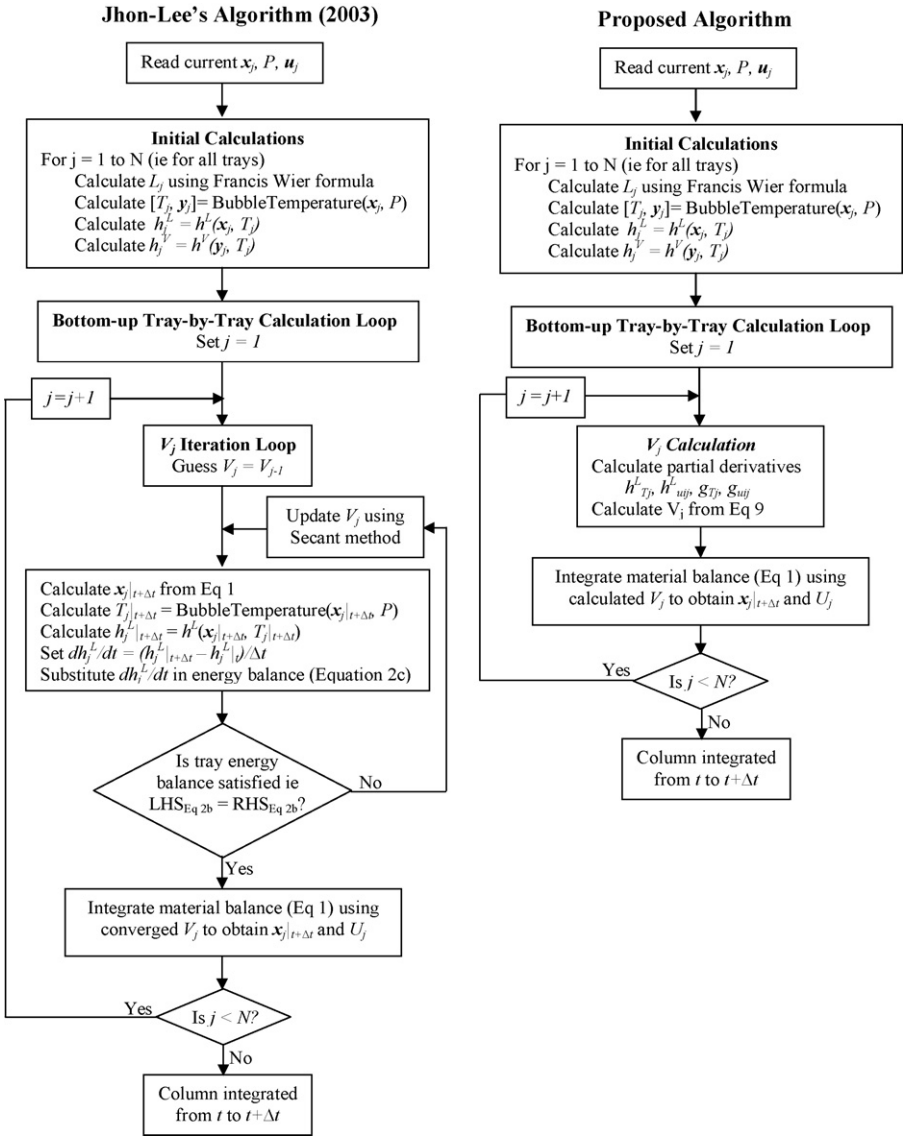

Fig. 2. Flowchart of the RD dynamic simulation algorithm of Jhon and Lee (2003) and the proposed algorithm.

3. Methyl acetate RD column

The reaction kinetics, VLE and enthalpy model details for simulating the methyl acetate RD column can be found in Singh et al. (2005). Briefly, an activity based kinetic expression is used. The Wilson equation models the liquid phase activity coefficient while the vapor phase is assumed ideal with Marek's correction accounting for vapor phase dimerization of acetic acid (Marek, 1955). The necessary modification in the analytical evaluation of dh_j^L/dt due to Marek's correction is briefly described in Appendix A. The liquid/vapor molar specific enthalpies are calculated from standard heat of formation data with excess enthalpy accounting for mixing heat effects. The liquid phase density is calculated from the Rackett equation. A schematic of the RD column is shown in Fig. 3. The basic design of the column is taken from Kumar and Kaistha (2008b) that minimizes the vapor boil-up. The column consists of 7 enriching, 26 reactive and 2 stripping trays. The column operating pressure is 1 atm with negligible pressure drop. The catalyst loading per reactive tray is 207.7 kg. The esterification reaction $MeOH + AcOH \leftrightarrow MeOAc + H_2O$ occurs on the reactive trays. Fresh acetic acid is fed just above the reactive zone at 300 kmol h^{-1}. Fresh methanol is fed at an equal stoichiometric rate (300 kmol h^{-1}) on Tray 11 into the reactive zone. Both the reactants are fed at their bubble points. For a reflux ratio of 1.5 and a distillate rate of 306.93 kmol h^{-1}, 95.8 mol% pure methyl acetate is recovered in the distillate stream. The corresponding reboiler duty is 3.4754 MW.

4. Results and discussion

In this section, the open loop and closed loop dynamic simulation results using the Jhon–Lee algorithm and the proposed algorithm are presented and compared in terms of the computational speed. The algorithms are coded in Visual Studio C++ version 9.0. Simple explicit Euler integration is used for integrating the tray-by-tray DAEs over time. A time step size of 2 s is used in all the results presented. For step sizes of 3 s and above, the Euler explicit integration is numerically unstable in case of the Jhon–Lee algorithm. For the proposed analytical scheme, even as the algorithm is numerically stable as higher time steps are used up to 6 s, the obtained dynamic response noticeably differs from the response using a 2-s time step. For smaller time steps, the obtained dynamic responses are very similar to the 2-s time step response in both the numerical and analytical algorithm simulations. A 2-s time-step thus represents a good accuracy versus simulation speed compromise.

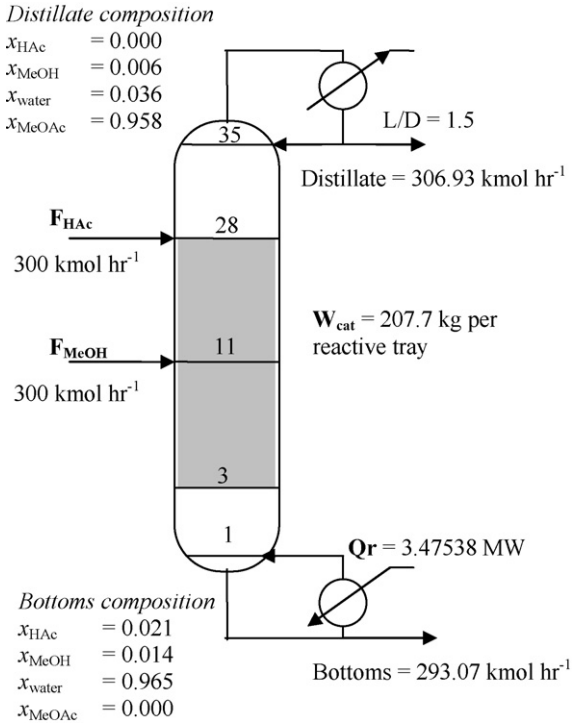

Fig. 3. Schematic of the methyl acetate RD column.

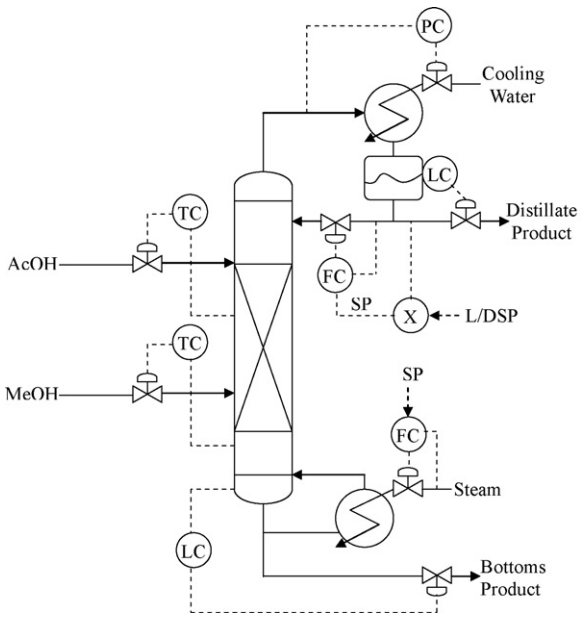

Fig. 4. Schematic of two-temperature control structure studied.

For closed loop operation, decentralized control using the two-point temperature inferential control structure originally proposed by Roat, Downs, Vogel, and Doss (1986) is applied. This structure has been chosen as in a recent study, Kaymak and Luyben (2005) found its control performance to be superior from amongst different two-point temperature control structures. The reader is referred to Al-Arfaj and Luyben (2002) and Kaymak and Luyben (2005) for a comprehensive evaluation of the other possible control structures. It is highlighted that temperature inferential control is preferred in the industry as the alternative of composition measurements is expensive and typically introduces large lags/dead time in the control loop.

A schematic of the studied control structure is shown in Fig. 4. A sensitive reactive tray temperature is controlled using the fresh acetic acid feed while a sensitive stripping tray temperature is controlled using the fresh methanol feed at constant reflux ratio. The reboiler duty (or vapor boil-up) acts as the through-put manipulator. From sensitivity analysis, tray temperature 5 (T_5) and tray temperature 2 (T_2) are found to be the most sensitive with respect to the fresh acetic acid (F_{HAc}) and fresh methanol (F_{MeOH}) feeds, respectively. Accordingly F_{HAc} controls T_5 while F_{MeOH} controls T_2. For tuning the temperature loops, the Tyreus–Luyben settings are obtained from the relay-feedback test and then appropriately detuned for a reasonable closed loop response to a ±20% step

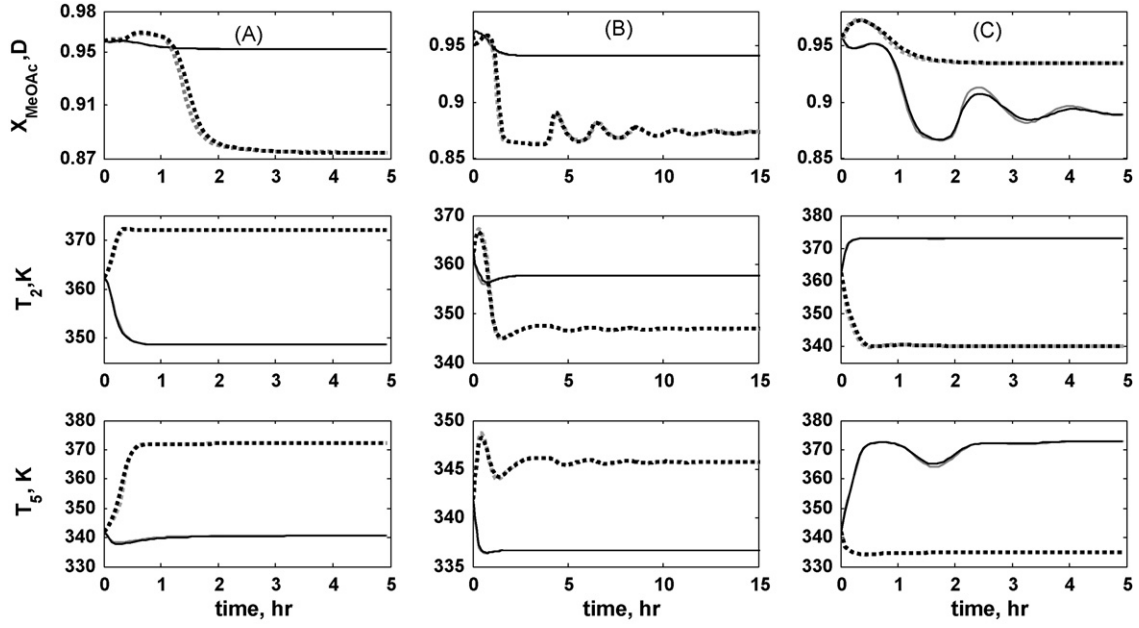

Fig. 5. Open loop response of distillate methyl acetate purity and controlled tray temperatures to ±20% step change in column inputs. (A) F_{MeOH}, (B) F_{AcOH} and (C) Q_r. Solid line: +20%; Grey: proposed algorithm. Broken line: −20%; Black: Jhon–Lee algorithm.

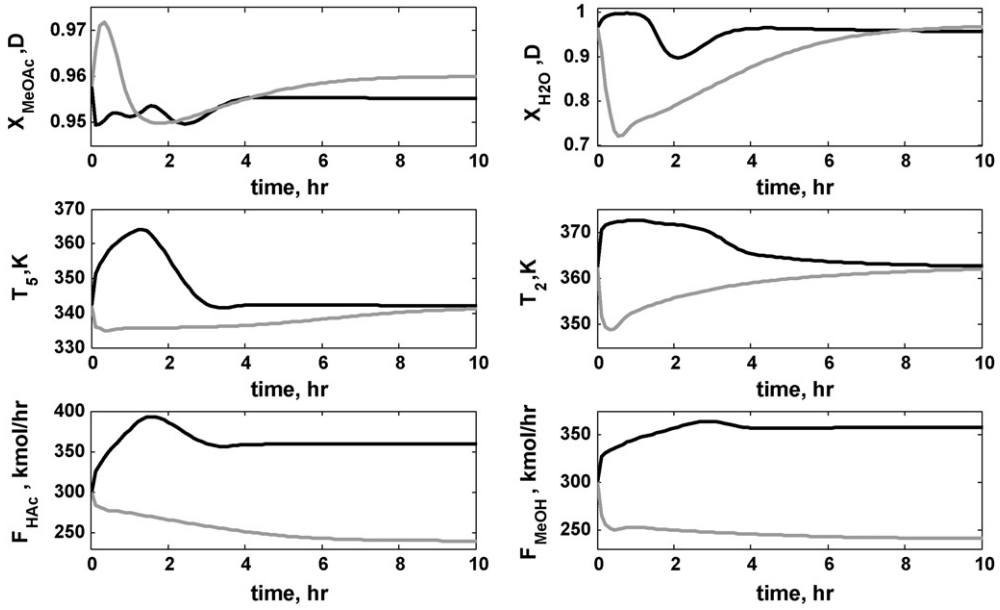

Fig. 6. Closed loop response to a ±20% step change in through-put. Black line: +20%; Grey line: −20%.

change in the process through-put, the principal disturbance into the column.

4.1. Open loop and closed loop results

Fig. 5 compares the open loop response of T_2, T_5 and the distillate methyl acetate purity ($x_{\mathrm{MeOAc}}{}^{\mathrm{D}}$) to a ±20% step change in either fresh feed and in the reboiler duty (Q_r) from the proposed analytical algorithm and the Jhon–Lee algorithm. The dynamic responses from the two algorithms are seen to be in good agreement. High non-linearity is also evident from the plots with significant asymmetry in the +20% and −20% input change responses. In particular, notice that the final steady state temperature of Tray 2 is below its base case temperature for *both* a 20% increase and a 20% decrease in F_{HAc} suggesting the presence of input multiplicity. Input multiplicity is also evident in the distillate purity response. The non-linearity is very typical of RD systems (Kumar & Kaistha, 2008c; Sneesby, Tade, & Smith, 1998).

Fig. 6 plots the closed loop response to a ±20% step change in Q_r, the through-put manipulator obtained proposed analytical algorithm. Closed loop results from the Jhon–Lee algorithm were found to be in very good agreement (data not shown). From the figure, the response completion time is about 10 h for a ±20% through-put change. Asymmetry in the response to a through-put change in opposite directions is evident from the figure. This may be attributed to non-linear effects. Also notice from the product purity response that the final steady-state distillate methyl acetate purity differs slightly from its base-case value. This is most probably due to column operation in the kinetically controlled regime. On-spec distillate purity would require control tray temperature set-point compensation (Kumar & Kaistha, 2008d).

4.2. Comparison of computational speed

The primary advantage of the proposed analytical algorithm is that the rate of change of tray molar specific enthalpy is directly obtained analytically and iterations requiring repeated bubble-point calculations as well as the one-step forward material balance integration for a numerical estimate of the same are avoided. The proposed analytical algorithm should thus be significantly faster than the Jhon–Lee numerical algorithm.

From Fig. 2, the algorithm consists of three main steps, namely, (i) initial calculations, (ii) V_j calculation and (iii) material balance integration. These steps are performed repeatedly at each integration time step so that the total CPU time taken for a step over the course of the dynamic simulation can be used to compare the computational speed of the two studied algorithms. The CPU time for these steps is obtained using the clock command in C++. For the two algorithms, the total CPU time for steps (i) and (iii) above were found to be similar as these steps are common to both the algorithms. A significant reduction in the total CPU time for the V_j calculation step (step (iii)) using the proposed algorithm was observed with consequent reduction in the overall simulation time.

To quantify the computational speed enhancement, Table 1 compares the CPU time for the V_j calculation step as well as for the overall simulation for 20 h dynamic simulations of the open loop and closed loop response reported in the previous section. These simulations were performed on an Intel Core 2 Duo CPU 2.83 GHz machine with 4GB RAM. From the data in the table, note that the V_j calculation step accounts for 70–75% of the total simulation time in the Jhon–Lee algorithm. The proposed analytical algorithm significantly speeds up the V_j calculation step by 3.5–5 times so that V_j calculation then consumes only about 20–30% of the total simulation time. The significant enhancement in the V_j calculation speed using the proposed algorithm translates to a 2–2(1/2)-fold increase in the overall simulation speed compared to the Jhon–Lee algorithm. The proposed algorithm is thus about twice (or more) as fast as the existing numerical algorithm.

To further analyze for the dependence of computational speed on the severity of the transient, Table 2 reports for the two algorithms, the total CPU time taken and the time taken for V_j calculation as the dynamic simulation time is increased from 1 to 20 h for a closed loop +20% through-put step change simulation. From the table, notice that the ratio of the V_j calculation time for the Jhon–Lee algorithm to that of the proposed algorithm monotonically decreases from 12 in the initial 1 h transient period to 5 for the complete 20 h transient period. Given that the severity of the transients is much more in the initial period (see Fig. 6), the data in the table suggests that the computational speed enhancement using the proposed algorithm over the Jhon–Lee algorithm increases with transient severity. This is because in the latter, the more severe the transient, the higher the number of iterations in the V_j calculation

Table 1
Computational speed comparison of V_j calculation step and complete simulation for methyl acetate column simulation[a] using the Jhon–Lee and proposed algorithms.

Input change description	V_j calculation step			Complete simulation		
	CPU time[b] Jhon–Lee algorithm	CPU time[b] proposed algorithm	Acceleration factor[c]	CPU time[b] Jhon–Lee algorithm	CPU time[b] proposed algorithm	Acceleration factor[c]
Open loop step response simulations						
F_{MeOH}						
+20%	200,150	55,495	3.61	277,515	141,344	1.96
−20%	214,738	56,509	3.80	295,969	147,563	2.01
F_{HAc}						
+20%	215,239	56,266	3.83	294,922	149,922	1.97
−20%	271,316	57,878	4.69	359,657	166,156	2.16
Q_r						
+20%	249,861	56,712	4.41	334,008	151,860	2.20
−20%	229,700	56,982	4.03	310,204	149,234	2.08
Closed loop through-put step response simulations						
Q_r						
+20%	305,286	61,613	4.95	399,937	158,562	2.52
−20%	286,668	62,266	4.60	380,078	161,203	2.36

[a] All simulation runs are for 20 h.
[b] Milliseconds, obtained using clock subroutine in C++.
[c] Ratio of Jhon–Lee CPU time to proposed algorithm CPU time.

Table 2
Comparison of CPU time[a] with respect to simulation time for Jhon–Lee and proposed algorithms for closed loop +20% through-put change methyl acetate RD simulation.

Simulation time	V_j calculation step			Complete simulation		
	CPU time Jhon–Lee algorithm	CPU time proposed algorithm	Acceleration factor[b]	CPU time Jhon–Lee algorithm	CPU time proposed algorithm	Acceleration factor[b]
1 h	39,710	3,203	12.40	45,390	8,875	5.11
5 h	117,030	15,879	7.37	145,188	43,360	3.35
10 h	191,800	31,593	6.07	244,609	83,078	2.94
15 h	250,867	46,164	5.43	324,171	121,765	2.66
20 h	305,286	61,613	4.95	399,937	158,562	2.52

[a] Milliseconds, obtained using clock subroutine in C++.
[b] Ratio of Jhon–Lee CPU time to proposed algorithm CPU time.

loop performing a bubble point calculation and a one-step forward material balance integration. The proposed algorithm, on the other hand, obtains V_j directly so that the V_j calculation is independent of transient severity and the total CPU time for V_j calculation scales linearly with simulation time. The same may be verified through a closer examination of column 3 in Table 2.

The CPU time results in Tables 1 and 2 clearly demonstrate a significant improvement by a factor of 2 or more, in the computational speed of solving the rigorous RD DAE model using the proposed algorithm. This can have potentially significant implications on non-linear model predictive control (MPC) and real-time optimization (RTO) of RD columns. Consider, for example, temperature set-point adjustment based on an estimate of the product composition and/or reaction conversion with the estimate being obtained from a rigorous non-linear model such as the one presented here. The frequency of set-point adjustment would typically be set by the computational time taken by the RTO/MPC optimizer, with repeated rigorous dynamic simulations constituting a major fraction of the total optimization time. The significant enhancement in the dynamic simulation speed using the proposed algorithm then translates to a reduction in the optimization time so that the temperature set-point adjustment frequency can be increased with consequent improvement in the tightness of product purity and/or reaction conversion control. The presented algorithm should thus be of interest to both the academic and industrial communities.

5. Conclusion

In conclusion, the proposed analytical method for direct calculation of the rate of change of tray molar specific enthalpy and consequently the vapor rate leaving a tray, significantly improves the computational speed for solving the RD column DAE model compared to existing numerical schemes. Specifically, results for the methyl acetate example RD column show that the computational time for open-loop and closed loop simulations reduces to half of that using the iterative Jhon–Lee algorithm.

Acknowledgement

The financial support from the Department of Science and Technology, Government of India, is gratefully acknowledged.

Appendix A. Modified procedure for Marek's correction

In the studied methyl acetate RD system, acetic acid has a tendency for dimerizing in the vapor phase affecting the vapor–liquid equilibrium. To account for the same, Marek's correction factor (Marek, 1955) is used in the VLE expression for the jth tray as

$$y_{i,j} = \frac{\gamma_{i,j} x_{i,j} P_{i,j}^{sat}}{\xi_{i,j} P_j} \tag{A1}$$

For convenience, the tray subscript j is dropped in subsequent expressions. For an associating component A (acetic acid in this case), the correction factor is

$$\xi_A = \frac{1 + \left(1 + 4k_A P_A^{sat}\right)^{1/2}}{1 + [1 + 4kPy_A(2 - y_A)]^{1/2}} \tag{A2a}$$

while for a non-associating component N, it is

$$\xi_N = \frac{2\left\{1 - y_A + [1 + 4kPy_A(2 - y_A)]^{1/2}\right\}}{(2 - y_A)\left\{1 + [1 + 4kPy_A(2 - y_A)]^{1/2}\right\}} \tag{A2b}$$

where k and k_A are the dimerization equilibrium constant for A in the mixture and pure A, respectively. It is assumed that $k = k_A$.

The modified VLE expression affects the bubble point so that at the bubble point

$$g \equiv \sum_{i=1}^{C} \frac{\gamma_i x_i P_i^{sat}}{\xi_i P} - 1 = 0 \equiv \sum_{i=1}^{C} \frac{w_i}{\xi_i} - 1 = 0 \tag{A3}$$

with

$$w_i = \frac{\gamma_i x_i P_i^{sat}}{P} \tag{A4}$$

From Eqs. (A2a) and (A2b), note that ξ_i is a function of the vapor phase composition of the associating component and temperature so that

$$\xi_i = \xi_i\,(y_A(\boldsymbol{u}), T) \tag{A5}$$

From Eq. (A3), using succinct notation for partial derivatives, we have

$$g_T = \sum_{i=1}^{C} \frac{1}{\xi_i} w_T^i - \frac{w_i}{\xi_i^2} \xi_T^i \tag{A6}$$

and

$$g_{u_k} = \sum_{i=1}^{C} \left[\frac{1}{\xi_i} w_{u_k}^i - \frac{w_i}{\xi_i^2} \xi_{u_k}^i \right] \tag{A7}$$

Differentiating Eq. (A5) with respect to u_k and applying the chain rule gives

$$\xi_{u_k}^i = \xi_{y_A}^i \cdot y_{A\ u_k} \tag{A8}$$

The VLE expression for the associating component A gives

$$\xi_A y_A = w_A$$

Taking the partial derivative with respect to u_k on both sides and rearranging

$$y_{A\,u_k} = \frac{w_{u_k}^A}{\left[y_A \xi_{y_A}^A + \xi_A\right]} \tag{A9}$$

Combining (A6), (A8) and (A9)

$$g_{u_k} = \sum_{i=1}^{C} \left[\frac{1}{\xi_i} w_{u_k}^i - \frac{w_i}{\xi_i^2} \xi_{y_A}^i \frac{w_{u_k}^A}{y_A \xi_{y_A}^A + \xi_A} \right] \tag{A10}$$

In the partial derivative expressions for g_T and g_{uk} in Eqs. (A6) and (A10) respectively, ${\xi_T}^i$ and $\xi_{y_A}^i$ are easily obtained by differentiating Eqs. (2a), (2b) and (2c). Also, since w_i corresponds to the VLE expression for component i without Marek's correction, the partial derivatives with respect to temperature (w_T^i) and tray component hold-up (w_{uk}^i) are known. All the terms on the RHS of Eqs. (A6) and (A10) are thus known giving the modified analytical derivative g_T and g_{uk} for use in Eq. (8) to obtain dT_j/dt. Since Marek's correction only affects the bubble point calculation, this is the only modification to the procedure outlined in the paper.

References

Al-Arfaj, M. A., & Luyben, W. L. (2002). Comparative control study and ideal and methyl acetate reactive distillation. *Chemical Engineering Science*, *57*, 5039–5050.

Baur, R., Taylor, R., & Krishna, R. (2001). Dynamic behaviour of reactive distillation columns described by a non-equilibrium stage model. *Chemical Engineering Science*, *56*, 2085–2102.

Chen, F., Huss, R. S., Malone, M. F., & Doherty, M. F. (2002). Multiple steady states in reactive distillation: Kinetic effects. *Comparative Chemical Engineering*, *26*, 81–93.

Georgiadis, M. C., Schenk, M., Pistikopoulos, E. N., & Gani, R. (2002). The interactions of design control and operability in reactive distillation systems. *Comparative Chemical Engineering*, *26*, 735–746.

Howard, G. M. (1970). Unsteady state behavior of multicomponent distillation columns. *AIChE Journal*, *16*, 1022–1033.

Jacobs, R., & Krishna, R. (1993). Multiple solutions in reactive distillation for methyl-*tert* butyl ether synthesis. *Industrial & Engineering Chemistry Research*, *35*, 1706–1709.

Jhon, Y. H., & Lee, T. H. (2003). Dynamic simulation for reactive distillation with ETBE synthesis. *Separation and Purification Technology*, *31*, 301–317.

Kaymak, D., & Luyben, W. L. (2005). Comparison of two types of two-temperature control structures for reactive distillation. *Industrial & Engineering Chemistry Research*, *44*, 4625–4640.

Kumar, M. V. P., & Kaistha, N. (2008a). Steady-state multiplicity and its implications on the control of an ideal reactive distillation column. *Industrial & Engineering Chemistry Research*, *47*, 2778–2787.

Kumar, M. V. P., & Kaistha, N. (2008b). Internal heat integration and controllability of double feed reactive distillation columns. 2. Effect of catalyst redistribution. *Industrial & Engineering Chemistry Research*, *47*, 7304–7311.

Kumar, M. V. P., & Kaistha, N. (2008c). Role of multiplicity in reactive distillation control system design. *Journal of Process Control*, *18*, 692–706.

Kumar, M. V. P., & Kaistha, N. (2008d). Decentralized control of a kinetically controlled ideal reactive distillation column. *Chemical Engineering Science*, *63*, 228–243.

Luyben, W. L. (1992). *Practical distillation control*. Van Nostrand Reinhold Inc.

Marek, J. (1955). Vapor liquid equilibria in mixtures containing an associating substance. II. Binary mixtures of acetic acid at atmospheric pressure. *Collection of Czechoslovak Chemical Communications*, *20*, 1490–1496.

Mohl, K., Kienle, A., Gilles, E., Rapmund, P., Sundmacher, K., & Hoffmann, U. (1999). Steady-state multiplicities in reactive distillation column for the production of fuel ethers MTBE and TAME: Theoretical analysis and experimental verification. *Chemical Engineering Science*, *54*, 1029–1043.

Noeres, C., Kenig, E. Y., & Górak, A. (2003). Modelling of reactive separation processes: reactive absorption and reactive distillation. *Chemical Engineering and Processing*, *42*, 157–178.

Roat, S., Downs, J., Vogel, E., & Doss, J. (1986). Integration of rigorous dynamic modeling and control synthesis for distillation columns. In M. Morari & T. J. McAvoy (Eds.), *Chem. Proc. Cont. III*. Amsterdam: Elsevier.

Seader, J. D., & Henley, E. J. (1998). *Separation process principles*. John Wiley.

Singh, B. P., Singh, R., Kumar, M. V. P., & Kaistha, N. (2005). Steady state analysis of reactive distillation using homotopy continuation method. *Chemical Engineering Research & Design*, *83A*, 959–968.

Sneesby, M. D., Tade, M. O., & Smith, T. N. (1998). Steady-state transitions in the reactive distillation of MTBE. *Comparative Chemical Engineering*, *22*, 879–892.